

2023-06-28

## An Aptamer-Based Microelectrode with Tunable Linear Range for Monitoring of K<sup>+</sup> in the Living Mouse Brain

Yuan-Dong Liu

Jia-Run Li

Li-Min Zhang

*Shanghai Key Laboratory of Green Chemistry and Chemical Processes, Department of Chemistry, School of Chemistry and Molecular Engineering, East China Normal University, Shanghai 200241, China, lmzhang@chem.ecnu.edu.cn*

Yang Tian

*Shanghai Key Laboratory of Green Chemistry and Chemical Processes, Department of Chemistry, School of Chemistry and Molecular Engineering, East China Normal University, Shanghai 200241, China, ytian@chem.ecnu.edu.cn*

---

### Recommended Citation

Yuan-Dong Liu, Jia-Run Li, Li-Min Zhang, Yang Tian. An Aptamer-Based Microelectrode with Tunable Linear Range for Monitoring of K<sup>+</sup> in the Living Mouse Brain[J]. *Journal of Electrochemistry*, 2023 , 29(6): 2218004.

DOI: 10.13208/j.electrochem.2218004

Available at: <https://jelectrochem.xmu.edu.cn/journal/vol29/iss6/13>

This Article is brought to you for free and open access by Journal of Electrochemistry. It has been accepted for inclusion in Journal of Electrochemistry by an authorized editor of Journal of Electrochemistry.

## ARTICLE

# An Aptamer-based Microelectrode with Tunable Linear Range for Monitoring of $K^+$ in the Living Mouse Brain

Yuan-Dong Liu<sup>#</sup>, Jia-Run Li<sup>#</sup>, Li-Min Zhang<sup>\*</sup>, Yang Tian<sup>\*</sup>

Shanghai Key Laboratory of Green Chemistry and Chemical Processes, Department of Chemistry, School of Chemistry and Molecular Engineering, East China Normal University, Shanghai, 200241, China

## Abstract

Potassium ion ( $K^+$ ) is widely involved in several physiopathological processes, and its abnormal changes are closely related to the occurrence of brain diseases of cerebral ischemia. *In vivo* acquirement of  $K^+$  variation is significant to understand the roles of  $K^+$  playing in brain functions. A microelectrode based on single-stranded DNA aptamers was developed for highly selective detection of  $K^+$  in brain, in which the aptamer probes were designed to contain an aptamer part for specific recognition of  $K^+$ , an alkynyl group used for stable confinement of aptamer probe on the gold surface, and an electrochemical redox active ferrocene group to generate current response signal. The response range of the microelectrodes could be rationally tuned by varying the chain length of the aptamer probe. The optimized electrode, LAC, displayed high selectivity for *in vivo* detection of  $K^+$ , and suitable linear range from  $10 \mu\text{mol}\cdot\text{L}^{-1}$ – $10 \text{mmol}\cdot\text{L}^{-1}$ , which could fulfill the requirement of  $K^+$  detection in brain. Eventually, the microelectrodes were successfully applied for the detection of  $K^+$  in the living mouse brains followed by hypoxic.

**Keywords:** Aptamer; Functional microelectrode; Potassium ion; Brain

## 1. Introduction

As the major cation of intracellular fluid, potassium ion ( $K^+$ ) is widely involved in neural signaling and physiopathological processes such as redox in the brain [1,2]. Abnormal changes of  $K^+$  concentration may be closely associated with a number of brain diseases, for example, cerebral ischemia and hemorrhage [3,4]. To date, the detection methods for  $K^+$  include atomic absorption spectroscopy [5], atomic emission spectroscopy [6], fluorescence spectroscopy [7] and so on. However, these methods are difficult to realize the *in vivo* detection of  $K^+$  in brain. Electrochemical methods with an implantable microelectrode are widely used for ion monitoring *in vivo* due to the advantages of high spatial and temporal resolutions [8–13]. However, the external electronic structure of  $K^+$  is similar to

that of sodium ion ( $\text{Na}^+$ ) and the concentration of extracellular  $\text{Na}^+$  is 30–50 times higher than that of  $K^+$  [14]. Therefore, identifying and detecting  $K^+$  with high selectivity in the living animals remains a great challenge (see Scheme 1).

Aptamers are single-stranded oligonucleotide molecules that can be screened *in vitro* for highly selective binding to a wide range of target analytes including ions, small molecules, proteins and peptides, and even whole cells [15–18]. By triggering the spatial folding of the aptamer upon binding to an ion, selective detection of  $K^+$  has been successfully achieved based on the signal variation depending on the distance between electrochemical response element and electrode surface [19]. Unfortunately, the developed aptamer-based electrochemical ion sensors generally possess the linear range from  $\text{nmol}\cdot\text{L}^{-1}$

Received 14 November 2022; Received in revised form 12 May 2023; Accepted 15 May 2023  
Available online 20 May 2023

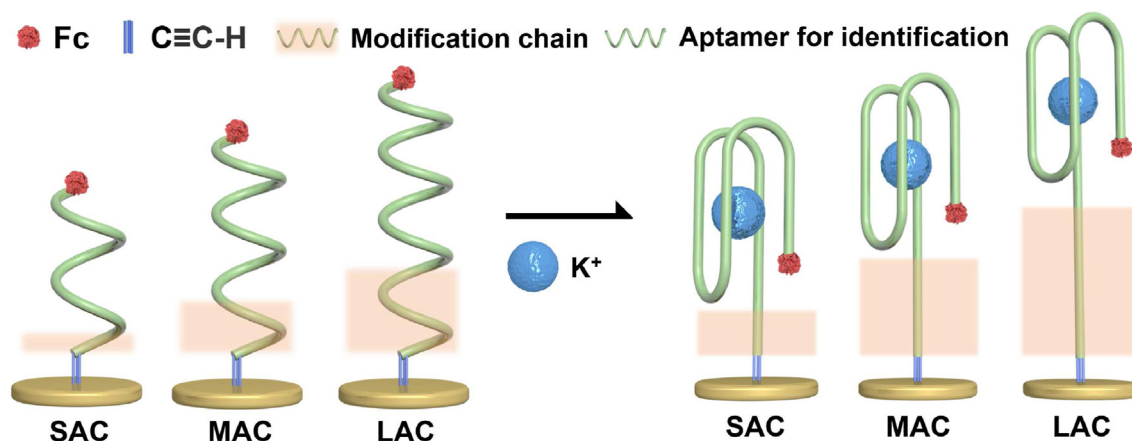
<sup>#</sup>These authors contributed equally to this work.

<sup>\*</sup> Corresponding author, Li-Min Zhang, E-mail address: [lmzhang@chem.ecnu.edu.cn](mailto:lmzhang@chem.ecnu.edu.cn).

<sup>\*</sup> Corresponding author, Yang Tian, E-mail address: [ytian@chem.ecnu.edu.cn](mailto:ytian@chem.ecnu.edu.cn).

<https://doi.org/10.13208/j.electrochem.2218004>

1006-3471/© 2023 Xiamen University and Chinese Chemical Society. This is an open access article under the CC BY 4.0 license (<https://creativecommons.org/licenses/by/4.0/>).



Scheme 1. The schematic diagram of working principle of microelectrode.

to  $\mu\text{mol}\cdot\text{L}^{-1}$ , which cannot fulfill the requirements for  $\text{K}^+$  with the level of  $\text{ca. mmol}\cdot\text{L}^{-1}$  in living rat brains. Thus, how to regulate the response of the aptamer-based electrode for *in vivo* application is still challenging.

To address these challenges, herein, an aptamer-modified microelectrode with a controlled linear range was designed and fabricated for the real-time detection of  $\text{K}^+$  in living brain through rationally tuning the distance of response to electrode surface. The aptamer TTTGGTTGGTGGTTGGTTT part was used to specific recognition of  $\text{K}^+$ , in which the electrochemical redox pair ferrocene was modified at the 5' end of the aptamer as an electrochemical redox group, and the alkyne group was modified at the 3' end to stably attach the aptamer to the surface of a carbon fiber electrode modified with gold particles. After recognition and capture of  $\text{K}^+$ , the aptamer folded conformationally to pull the Fc group closer to the electrode surface, generating the increasing of faradic current response. On the other hand, to regulate the linear range of the microelectrode in a controlled manner, we designed different modified chain lengths of the aptamer to vary the distance between the Fc and the electrode surface after folding with  $\text{K}^+$ , which effectively changed the linear range of the microelectrode and made the microelectrode suitable for *in vivo* brain detection (Scheme 1). Eventually, based on a tunable electrochemical sensor, we successfully achieved the measurement of  $\text{K}^+$  in the mouse brain under hypoxia.

## 2. Experimental section

### 2.1. Chemicals and reagents

Carbon fibers were purchased from Tokai Carbon Co. (Tokai, Japan).  $\text{AuCl}_3\cdot\text{HCl}\cdot 4\text{H}_2\text{O}$ ,  $\text{K}_3[\text{Fe}(\text{CN})_6]$ ,  $\text{NaCl}$ ,  $\text{CaCl}_2$ ,  $\text{KCl}$ ,  $\text{MgCl}_2\cdot 6\text{H}_2\text{O}$ ,

$\text{CuCl}_2\cdot 2\text{H}_2\text{O}$ ,  $\text{FeCl}_3\cdot 6\text{H}_2\text{O}$ ,  $\text{ZnCl}_2$ ,  $\text{AlCl}_3\cdot 6\text{H}_2\text{O}$ , Ascorbic acid (AA), dopamine (DA), uric acid (UA), Cysteine (Cys), glutamine (Gln), Histidine (His) and arginine (Arg) were purchased from Aladdin Chemistry Co. Ltd. (Shanghai, China). Artificial cerebrospinal fluid (aCSF) powder was purchased from Adamas-Beta (Shanghai, China).  $\text{C}\equiv\text{C}-\text{H}$  and ferrocene (Fc) double modified aptamers [17] were synthesized by Shanghai DNA Bioscience Co.Ltd. Chooses the sequence of SAC:  $\text{Fc}-5'-\text{TTTGGTTGGTGTGGTTGGTTT}-3'-\text{C}\equiv\text{C}-\text{H}$ , MAC:  $\text{Fc}-5'-\text{TTTGGTTGGTGTGGTTGGTTT}-3'-\text{C}\equiv\text{C}-\text{H}$ , LAC:  $\text{Fc}-5'-\text{TTTGGTTGGTGTGGTTGGTTT}-3'-\text{C}\equiv\text{C}-\text{H}$ .

### 2.2. Preparation of microelectrodes

Carbon fiber microelectrodes (CFME) were prepared as previously described [20,21] and soaked in acetone to clean the surface before use. Subsequently, gold micro-sheets were surface modified by CFME electrodeposition in  $0.1\text{ mol}\cdot\text{L}^{-1}$   $\text{HAuCl}_4$  solution at  $-0.2\text{ V}$  vs.  $\text{Ag}/\text{AgCl}$  for 10 s. The electrode was rinsed with water to remove the attached solution and then dried under  $\text{N}_2$  for 6 h.

### 2.3. Modification of aptamers onto electrode surfaces

The  $\text{C}\equiv\text{C}-\text{H}$  and ferrocene (Fc) double modified aptamers were prepared in  $100\text{ }\mu\text{mol}\cdot\text{L}^{-1}$  aqueous solution with  $\text{N}_2$  to remove the  $\text{O}_2$  dissolved in water. Then, the prepared  $\text{AuS}/\text{CFME}$  was immersed in aptamer solution for 6 h at  $60\text{ }^\circ\text{C}$  to modify the aptamer on the electrode surface [22].

### 2.4. The *in vivo* mice cerebral hypoxia experiments

All animal experiments were performed according to the guidelines of the Care and Use of Laboratory Animals formulated by the Ministry of

Science and Technology of China, and were approved by the Animal Care and Use Committee of East China Normal University (the approval no. m<sup>+</sup> R20190304, Shanghai, China). To achieve the detection of K<sup>+</sup> in the hippocampal region of the brain of living mice, C57BL/6 mice were anesthetized with 2% isoflurane. The mice were then fixed on a brain stereotaxic instrument and the scalp was cleaned of connective tissue after incision with scissors. The skull surface of the brain was then placed to the midline bregma position at AP = -1.30 mm, L = 0.75 mm anterior to bregma, and V = 1.25 mm from the surface. A small hole was drilled in the surface of the skull. The microelectrodes were carefully implanted into the brain. Hypoxia experiments were performed by placing the mice in a homemade gas-tight box with a flowing gas mixture (5% O<sub>2</sub> and 95% N<sub>2</sub>).

### 3. Results and discussion

Carbon fibers with good electrical conductivity and biocompatibility were chosen as the substrate to fabricate the functional microelectrodes (CFME) (Fig. 1A). The dense gold micro-sheets were in situ electrodeposited on the CFME surface, which is denoted as AuS/CFME (Fig. 1B and C). The reduction peak of AuS/CFME in the cyclic

voltammetric (CV) curve in 0.01 mol·L<sup>-1</sup> H<sub>2</sub>SO<sub>4</sub> at ca. 0.9 V (vs. Ag/AgCl) could be used to calculate the charge consumption (Fig. 1D). The electroactive area of the electrode can be estimated using the following equation [22],

$$A = Q/386$$

in which  $Q$  is the charge consumed, and  $Q = 386$  ( $\mu\text{C}\cdot\text{cm}^{-2}$ ) per unit area of the clean Au electrode. The calculated electrochemical active area of AuS/GO was 0.05 cm<sup>2</sup>, which is ca. 7.8 times larger than the geometric area of bare CFME. The CV curves in 1.0 mmol·L<sup>-1</sup> K<sub>3</sub>[Fe(CN)<sub>6</sub>] (Fig. 2) show a “S” characteristic current peak pattern, demonstrating the typical microelectrode feature. Moreover, the ultimate diffusion current of AuS/CFME was 2.4 times larger than that of bare CFME, which might be originated from the enlarged electroactive surface area (Curve b in Fig. 2).

Previous investigation has reported that under physiological conditions, the thiol ligands can be replaced by abundant biological thiol such as glutathione (GSH), resulting in detection of distortions and unstable adsorption of molecules onto the gold surfaces [23,24]. To solve this problem, the Au-C≡C bonding method has been recently developed to enhance the stability of molecular-assembly at electrode surface [22]. As a result, the

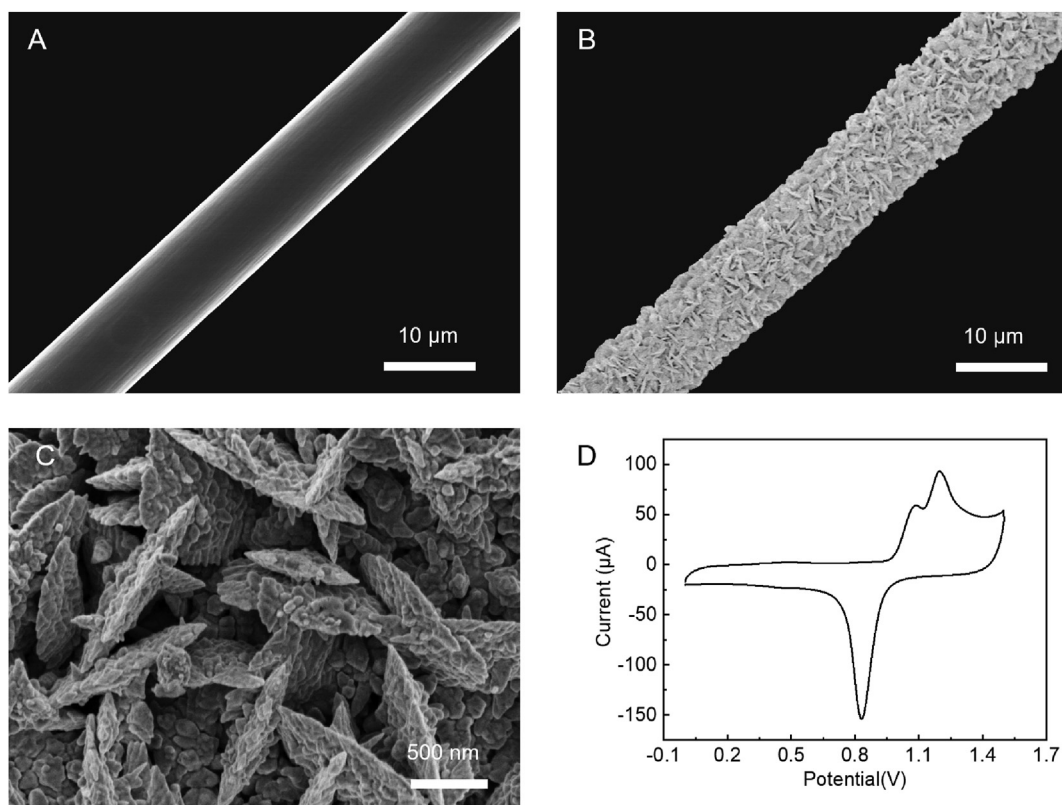


Fig. 1. SEM images of CFME (A) and AuS/CFME (B and C), and CV curve of AuS/CFME (D) in 0.01 mol·L<sup>-1</sup> H<sub>2</sub>SO<sub>4</sub> aqueous solution. Scan rate is 100 mV·s<sup>-1</sup>.

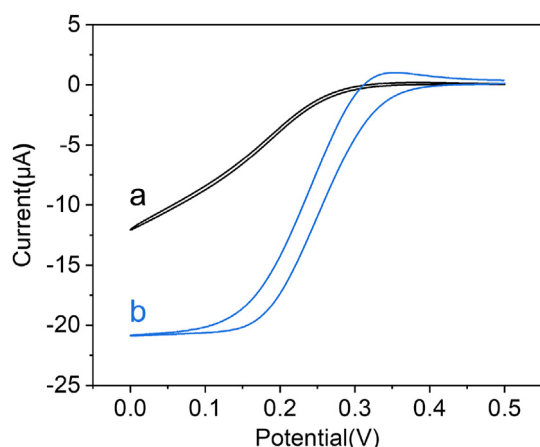


Fig. 2. CV curves of bare CFME (a) and AuS/CFME (b) in  $0.05 \text{ mol}\cdot\text{L}^{-1} \text{ K}_3[\text{Fe}(\text{CN})_6]$  solution. Scan rate is  $20 \text{ mV}\cdot\text{s}^{-1}$ .

alkyne group was selected and modified at the 3' end of the aptamer to attach the aptamer probe at AuS/CFME with high stability. Meanwhile, an electrochemical redox pair of ferrocenes (Fc) was modified at the 5' end of the aptamer to be used as an electrochemical response signal to indirectly reflect the variation of  $\text{K}^+$  concentrations. In order to rationally modulate the response range of the aptamer-based electrochemical sensors toward the application in brain, three aptamers with different chain lengths were designed and confined at Au nanoparticles modified CFME. The corresponding modified microelectrodes with different chain lengths are denoted as SAC (Fc-5'-TTTGGTTG GTGTGGTTGGTTT-3'-C≡C-H), MAC (Fc-5'-TTTGGTTGGTGTGGTTGGTTTTTTTTTTTTTTT-3'-C≡C-H) and LAC (Fc-5'-TTTGGTTGGTGTGGTTGGTTTTTTTTTTTTTTTTTTT-3'-C≡C-H). Infrared spectroscopy (Fig. 3) was used to track the modification of aptamer probes at AuS/CFME. The appearances of C-O bonds, C=O bonds and -OH originated from aptamers demonstrated the successful modification of aptamers on the AuS/CFME.

Next, differential pulse voltammetry (DPV) was employed to track the modification steps owing to its high sensitivity. As shown in Fig. 4, an anodic peak was observed at 0.22 V (vs. Ag/AgCl) in aCSF solution (pH 7.4) when SAC was modified at AuS/CFME, which is ascribed to the oxidation of Fc to  $\text{Fc}^+$ . Such anodic current signals of  $\text{Fc}/\text{Fc}^+$  were found to be strongly dependent on the chain length, which the largest current was determined at the SAC electrode (Curve a), but the current response was gradually decreased with the increasing chain length of aptamer modified at the AuS/CFME (Curves b and c). These results indicated that the longer aptamer-modified chain

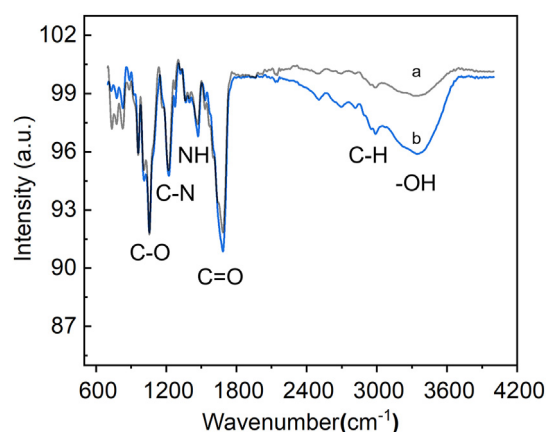


Fig. 3. Infrared spectra of SAC (a) and LAC (b).

lengths gave rise to the longer distance of  $\text{Fc}/\text{Fc}^+$  to underlying electrode surface, leading to the weakened current response.

Then, the DPV curves of different aptamer-electrodes were obtained in aqueous solution containing different  $\text{K}^+$  concentrations. As shown in Fig. 5, the peak current density ( $J_p$ ) obtained at SAC electrode gradually increased with the increasing of the  $\text{K}^+$  concentration. Similar increasing tendency of peak current on  $\text{K}^+$  concentrations was also observed at MAC and LAC electrodes. However, three kinds of aptamer-based microelectrodes exhibited the different linear current response ranges toward  $\text{K}^+$  concentrations, namely,  $0.3 \text{ nmol}\cdot\text{L}^{-1}$ – $100 \text{ nmol}\cdot\text{L}^{-1}$  for SAC (Fig. 4B),  $3.0 \text{ nmol}\cdot\text{L}^{-1}$ – $10 \text{ }\mu\text{mol}\cdot\text{L}^{-1}$  for MAC (Fig. 4D), and  $10 \text{ }\mu\text{mol}\cdot\text{L}^{-1}$ – $10 \text{ mmol}\cdot\text{L}^{-1}$  for LAC (Fig. 4F) electrodes. These results demonstrated that the response of aptamer-based electrode was strongly dependent on the concentrations of  $\text{K}^+$ , and the increasing of aptamer chain length could rationally regulate the sensitivity of the

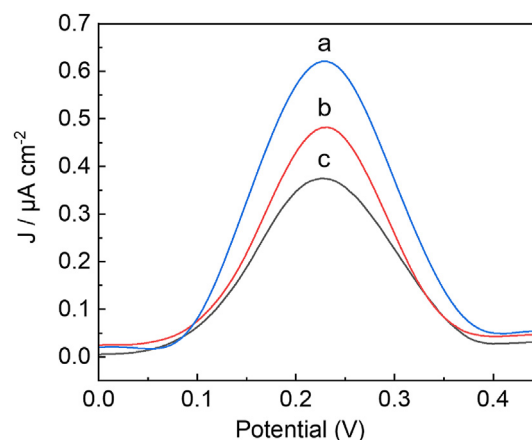


Fig. 4. CV curves obtained at SAC (a), MAC (b) and LAC (c) electrodes in blank aCSF solution (pH 7.4).

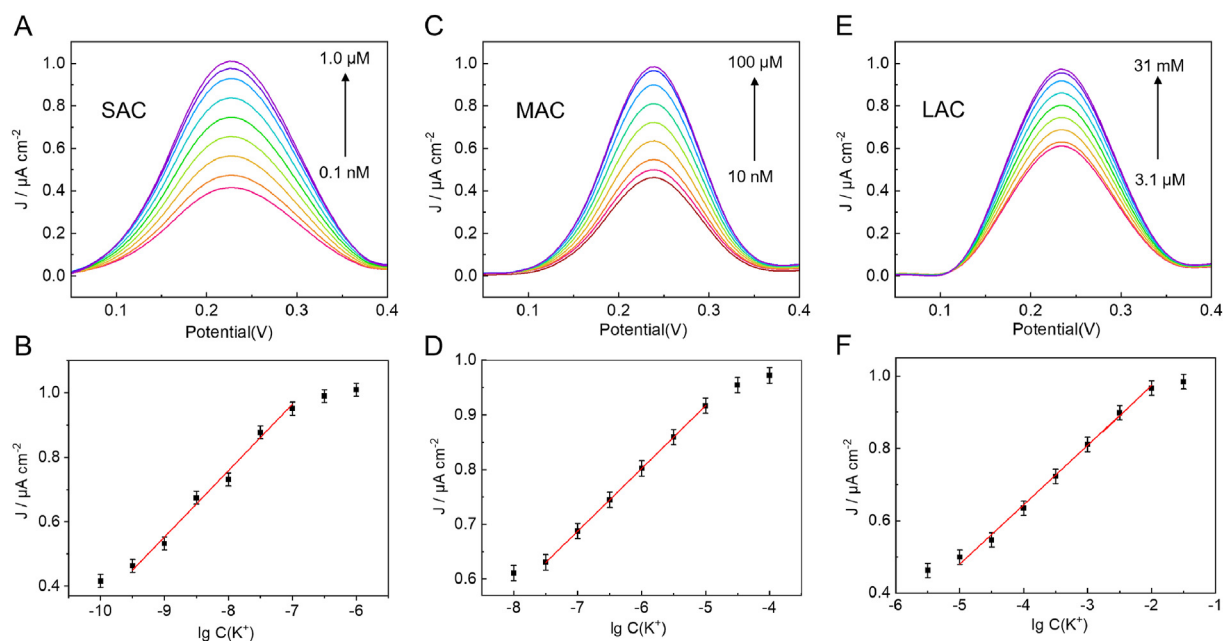


Fig. 5. CV curves obtained at SAC (A), MAC (C) and LAC (E) in aqueous solution after continuously adding different  $K^+$  concentrations, and the corresponding linear plots of current density versus  $K^+$  concentration obtained at SAC (B), MAC (D) and LAC (F).

electrochemical sensor toward higher concentration levels. Since the basal concentration of extracellular  $K^+$  in brain was approximately  $2.6 \text{ mmol}\cdot\text{L}^{-1}$ , the LAC was eventually optimized and selected as the electrochemical sensor for *in vivo* detection of  $K^+$  in the living brain.

Selectivity of electrochemical sensors is important for *in vivo* application in complex brain environments. Then, we performed the selectivity and competition tests of the LAC for potential interferences of co-existing various substances in practical brain systems, including metal ions ( $\text{Na}^+$ ,  $\text{Ca}^{2+}$ ,  $\text{Mg}^{2+}$ ,  $\text{Cu}^{2+}$ ,  $\text{Zn}^{2+}$  and  $\text{Al}^{3+}$ ), biological species (AA, DA and UA) and amino acids (Cys, Gln, His and Arg). The results showed that all the interferences were less than 3.5% (Fig. 6), demonstrating the high selectivity of the aptamer-modified microelectrode. In addition, the stability of the electrodes was also investigated. Two microelectrodes with alkyne- and sulfhydryl-modified aptamers were immersed in GSH solution ( $5 \text{ mmol}\cdot\text{L}^{-1}$ ) according to the living brain environment (Fig. 7A). It was found that the alkyne-modified microelectrode maintained 96.4% sensitivity, while the sulfhydryl-modified electrode only had 76.4% after immersing in GSH solution for 8 h. The results demonstrated the effectiveness of the alkyne-based modification method on gold surfaces against interference from other sulfhydryl-rich substances. Next, the temporal stability of the alkyne-modified microelectrodes LAC was also tested in the artificial cerebrospinal fluid (aCSF) without  $K^+$ . The results showed that the LAC

maintained 96.3% sensitivity after 12-h continuous immersion in aCSF, demonstrating the high stability of the LAC electrodes (Fig. 7).

To verify the feasibility of *in vivo* assays, LAC was optimized and used to record changes in extracellular  $K^+$  concentrations in the hippocampal region of the mouse brain before and after 10-min hypoxia (Fig. 8A). It was found that the  $K^+$  concentration in the hippocampus increased from  $2.6 \text{ mmol}\cdot\text{L}^{-1}$  to  $8.7 \text{ mmol}\cdot\text{L}^{-1}$  with the onset of brain hypoxia in mice for 10 min (Fig. 8B and C). Such variation might be caused by the depolarization of brain cells in the hypoxic environment

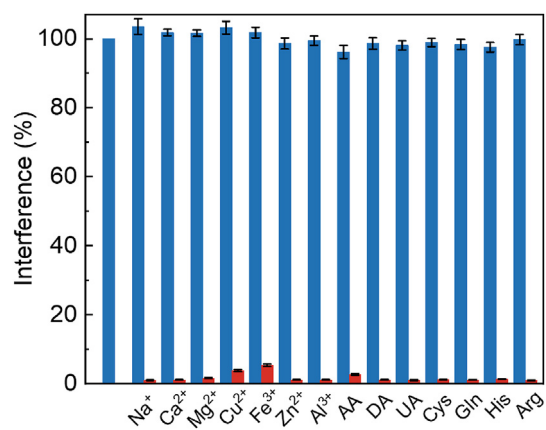


Fig. 6. Selective (Red) and competitive (Blue) tests obtained at LAC for determination of  $K^+$  against various potential interferences. The concentrations of  $K^+$  were  $1 \text{ mmol}\cdot\text{L}^{-1}$ ,  $\text{Ca}^{2+}$  and  $\text{Na}^+$  were  $1 \text{ mmol}\cdot\text{L}^{-1}$ , and  $\text{Cu}^{2+}$  and  $\text{Fe}^{3+}$  were  $1 \text{ }\mu\text{mol}\cdot\text{L}^{-1}$ , while other metal ions, neurotransmitters and amino acids were all  $10 \text{ }\mu\text{mol}\cdot\text{L}^{-1}$ .

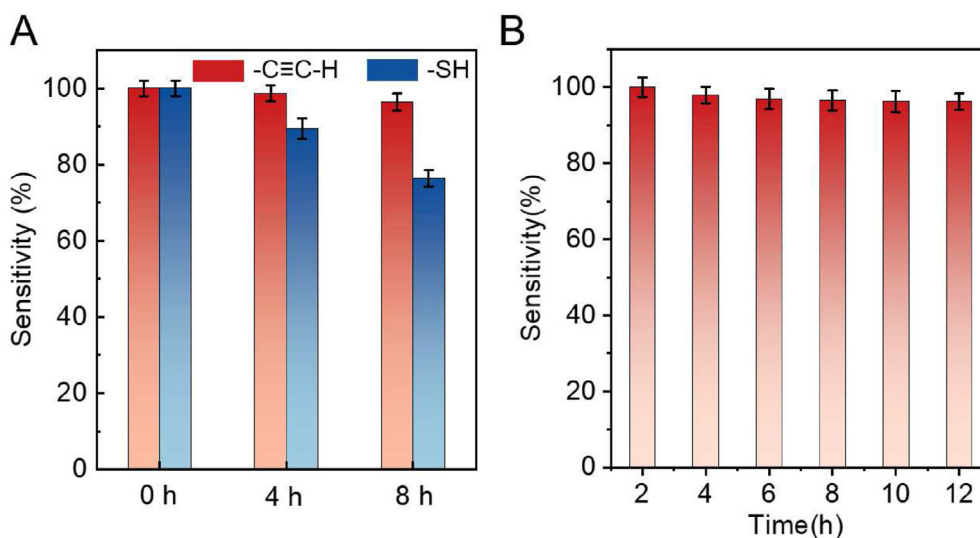


Fig. 7. (A) Sensitivity plots of LAC modified with  $-C\equiv C-H$  and  $-SH$  after being implanted in  $5 \text{ mmol}\cdot\text{L}^{-1}$  GSH solution for 4 and 8 h ( $n = 6$ , S.D.). (B) Sensitivity plots of LAC after being implanted in aCSF without  $K^+$  for 1–12 h ( $n = 6$ , S.D.). The sensitivity value was calculated based on the calibration plot obtained at LAC in aqueous solution containing  $K^+$  concentration ranging from  $100 \mu\text{mol}\cdot\text{L}^{-1}$  to  $1 \text{ mmol}\cdot\text{L}^{-1}$ .

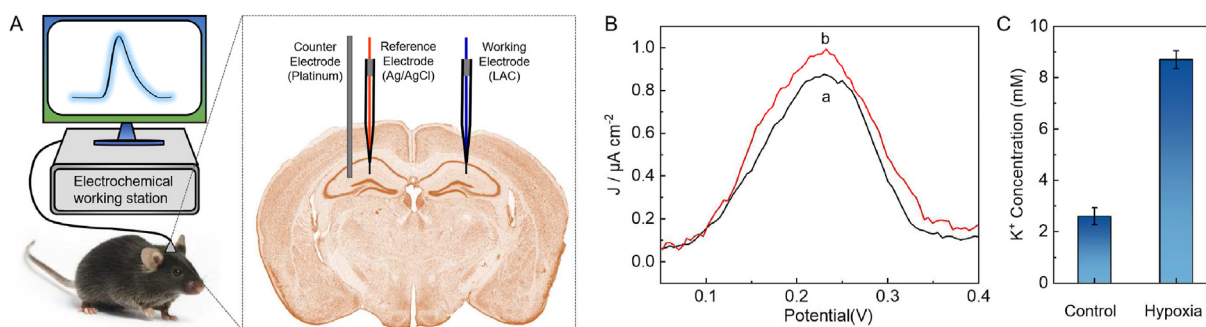


Fig. 8. (A) Schematic diagram of *in vivo* brain electrochemical monitoring in mouse brain. (B) Typical CV curves in hippocampus obtained at LAC in normal mouse brain (a), and mouse brain followed by hypoxic for 10 min (b), and (C) the corresponding estimated  $K^+$  concentration.

[20]. In order to verify the reliability of the results tested by the LAC electrode, we also sampled cerebrospinal fluid from the hippocampus of the mouse brain for testing in a blood gas analyzer, and found that the difference between the  $K^+$  concentrations obtained by our developed LAC electrode and blood gas analyzer was less than 4%, demonstrating the high accuracy of the developed LAC microelectrode.

#### 4. Conclusions

The aptamer-modified microelectrodes with a controlled linear range were designed and applied for the real-time detection of  $K^+$  in the living brain. Three  $K^+$  aptamers composed of different chain lengths were designed, in which the alkyne group at the 3' end to anchor the aptamer probe at the electrode surface, and the 5' segment with ferrocene was used as the electrochemical response signal for  $K^+$  variation. We found that the linear response range of  $K^+$  detection by the microelectrode

gradually shifted to higher concentrations as the length of the aptamer chain was increased. The LAC with the longest modified chain displayed a linear response in the range of  $10 \mu\text{mol}\cdot\text{L}^{-1}$ – $10 \text{ mmol}\cdot\text{L}^{-1}$ , which enable it to meet the testing requirements in the practical living brain. Finally, the LAC was demonstrated to be applicable for *in vivo*  $K^+$  detection in mouse brain followed by hypoxia. The developed strategy for rationally regulating the response range of the aptamer-modified sensor might pave a new way to broaden the application of the aptamer-modified sensor in different measurement systems, in particular, brain analysis.

#### Acknowledgements

This work was supported by the National Natural Science Foundation of China (22022402, 21974051 for L. Zhang and 22004037, 21635003, 21827814, and 21811540027 for Y. Tian) and the Innovation Program of Shanghai Municipal Education Commission (201701070005E00020) for Y. Tian. We also

greatly appreciate the Fundamental Research Funds for the Central Universities.

## References

- [1] Fahanik-Babaei J, Rezaee B, Nazari M, Torabi N, Saghiri R, Sauve R, Eliassi A. A new brain mitochondrial sodium-sensitive potassium channel: effect of sodium ions on respiratory chain activity[J]. *J. Cell Sci.*, 2020, 133(10): jcs242446.
- [2] Kamel H, Healey J. Cardioembolic stroke[J]. *Circ. Res.*, 2017, 120(3): 514–526.
- [3] Liu Y D, Liu Z C, Zhao F, Tian Y. Long-term tracking and dynamically quantifying of reversible changes of extracellular  $\text{Ca}^{2+}$  in multiple brain regions of freely moving animals[J]. *Angew. Chem. Int. Edit.*, 2021, 60(26): 14429–14437.
- [4] Weaver C M. Potassium and health[J]. *Adv. Nutr.*, 2013, 4(3): 368S–377S.
- [5] Qu Z, Steinvall E, Ghorbani R, Schmidt F M. Tunable diode laser atomic absorption spectroscopy for detection of potassium under optically thick conditions[J]. *Anal. Chem.*, 2016, 88(7): 3754–3760.
- [6] Beiraghi A, Shokri M. A novel task specific magnetic polymeric ionic liquid for selective preconcentration of potassium in oil samples using centrifuge-less dispersive liquid-liquid microextraction technique and its determination by flame atomic emission spectroscopy[J]. *Talanta*, 2018, 178: 616–621.
- [7] Jewell M P, Greer M D, Dailey A L, Cash K J. Triplet-triplet annihilation upconversion based nanosensors for fluorescence detection of potassium[J]. *ACS Sens.*, 2020, 5(2): 474–480.
- [8] Liu Y D, Liu Z C, Tian Y. Real-time tracking of electrical signals and an accurate quantification of chemical signals with long-term stability in the live brain[J]. *Acc. Chem. Res.*, 2022, 55(19): 2821–2832.
- [9] Da Y F, Luo S H, Tian Y. Real-time monitoring of neurotransmitters in the brain of living animals[J]. *ACS Appl. Mater. Interfaces*, 2022, 15(1): 138–157.
- [10] Liu Z C, Tian Y. Recent advances in development of devices and probes for sensing and imaging in the brain[J]. *Sci. China-Chem.*, 2021, 64(6): 915–931.
- [11] Huang S Q, Zhang L M, Dai L Y, Wang Y Y, Tian Y. Nonenzymatic electrochemical sensor with ratiometric signal output for selective determination of superoxide anion in rat brain[J]. *Anal. Chem.*, 2021, 93(13): 5570–5576.
- [12] Qian Y J, Zhang L M, Tian Y. Highly stable electrochemical probe with bidentate thiols for ratiometric monitoring of endogenous polysulfide in living mouse brains[J]. *Anal. Chem.*, 2022, 94(2): 1447–1455.
- [13] Dong H, Zhou Q, Zhang L M, Tian Y. Rational design of specific recognition molecules for simultaneously monitoring of endogenous polysulfide and hydrogen sulfide in the mouse brain[J]. *Angew. Chem. Int. Edit.*, 2019, 58(39): 13948–13953.
- [14] Zhao F, Liu Y D, Dong H, Feng S Q, Shi G Y, Lin L N, Tian Y. An electrochemophysiological microarray for real-time monitoring and quantification of multiple ions in the brain of a freely moving rat[J]. *Angew. Chem. Int. Edit.*, 2020, 59(26): 10426–10430.
- [15] Dunn M R, McCloskey C M, Buckley P, Rhea K, Chaput J C. Generating biologically stable TNA aptamers that function with high affinity and thermal stability[J]. *J. Am. Chem. Soc.*, 2020, 142(17): 7721–7724.
- [16] Stephens M. The emerging potential of Aptamers as therapeutic agents in infection and inflammation[J]. *Pharmacol. Ther.*, 2022, 238: 108173.
- [17] Gong Z W, Liu Z C, Zhang Z H, Mei Y X, Tian Y. A highly stable two-photon ratiometric fluorescence probe for real-time biosensing and imaging of nitric oxide in brain tissues and larval zebrafish[J]. *CCS Chemistry*, 2022, 4: 1–23.
- [18] Liu Z C, Zhu Y, Zhang L M, Jiang W P, Liu Y W, Tang Q W, Cai X Q, Li J, Wang L H, Tao C L, Yin X Z, Li X W, Hou S G, Jiang D W, Liu K, Zhou X, Zhang H J, Liu M L, Fan C H, Tian Y. Structural and functional imaging of brains[J]. *Sci. China-Chem.*, 2022, 66(2): 324–366.
- [19] Chen Z B, Guo J X, Zhang S G, Chen L. A one-step electrochemical sensor for rapid detection of potassium ion based on structure-switching aptamer[J]. *Sens. Actuator B-Chem.*, 2013, 188: 1155–1157.
- [20] Zhang L M, Tian Y. Designing recognition molecules and tailoring functional surfaces for in vivo monitoring of small molecules in the brain[J]. *Accounts Chem. Res.*, 2018, 51(3): 688–696.
- [21] Liu W, Dong H, Zhang L M, Tian Y. Development of an efficient biosensor for the in vivo monitoring of  $\text{Cu}^{+}$  and pH in the brain: rational design and synthesis of recognition molecules[J]. *Angew. Chem. Int. Edit.*, 2017, 56(51): 16328–16332.
- [22] Zhang C P, Liu Z C, Zhang L M, Zhu A W, Liao F M, Wan J J, Zhou J, Tian Y. A robust  $\text{Au-C}\equiv\text{C}$  functionalized surface: toward real-time mapping and accurate quantification of  $\text{Fe}^{2+}$  in the brains of live ad Mouse models[J]. *Angew. Chem. Int. Edit.*, 2020, 59(46): 20499–20507.
- [23] Gao X, Jiang L, Hu B, et al. Au-Se bond based nanoprobe for imaging MMP-2 in Tumor cells under a high-thiol environment[J]. *Anal. Chem.*, 2018, 90(7): 4719–4724.
- [24] Liu H, Radford M N, Yang C T, Chen W, Xian M. Inorganic hydrogen polysulfides: Chemistry, chemical biology, and detection[J]. *Br. J. Pharmacol.*, 2019, 176(4): 616–627.



# 基于线性范围可调的适配体功能化微电极的鼠脑中钾离子的活体分析

刘原东<sup>#</sup>, 李佳润<sup>#</sup>, 张立敏<sup>\*</sup>, 田 阳<sup>\*</sup>

化学与分子工程学院, 华东师范大学, 上海 200241, 中国

## 摘要

钾离子 ( $K^+$ ) 广泛参与多种生理病理过程, 其异常变化与脑缺血等脑部疾病的发生密切相关。在体内获取  $K^+$  的变化对了解  $K^+$  在大脑功能中发挥的作用具有重要意义。我们开发了一种基于单链 DNA 诱导结构变化的微电极, 用于高选择性地检测大脑中的  $K^+$ 。电化学探针主要由三部分组成, 其中适配体片段用于特异性识别  $K^+$ , 末端炔基基团用于高稳定组装探针于金表面, 头部修饰的二茂铁基团作为电化学活性基团提供响应信号。结果表明通过合理地调控适配体的烷基链的长度, 可以有效调节微电极的线性响应区间。其中优化后的电极 LAC 电极对  $K^+$  检测体现出了高的选择性, 在  $10 \mu\text{mol}\cdot\text{L}^{-1}$ – $10 \text{mmol}\cdot\text{L}^{-1}$  的线性范围展示了良好的线性关系。最终该新型微电极被成功应用于活体小鼠大脑中  $K^+$  的实时检测。

**关键词:** 适配体; 微电极; 钾离子; 脑